Supplementary Information

EXP2 is a nutrient-permeable channel in the vacuolar membrane of *Plasmodium* and is essential for protein export via PTEX

Matthias Garten[1], Armiyaw S. Nasamu[2], Jacquin C. Niles[3], Joshua Zimmerberg[1*], Daniel E. Goldberg[2*], and Josh R. Beck[2,4]

[1]Section on Integrative Biophysics, Eunice Kennedy Shriver National Institute of Child Health and Human Development, National Institutes of Health, Bethesda, MD, 20892, USA

[2]Departments of Medicine and Molecular Microbiology, Washington University School of Medicine, St. Louis, MO 63110, USA

[3]Department of Biological Engineering, Massachusetts Institute of Technology, Cambridge, MA 02139, USA

[4]Department of Biomedical Sciences, Iowa State University, Ames, IA 50011 USA

*email: dgoldberg@wustl.edu and zimmerbj@mail.nih.gov

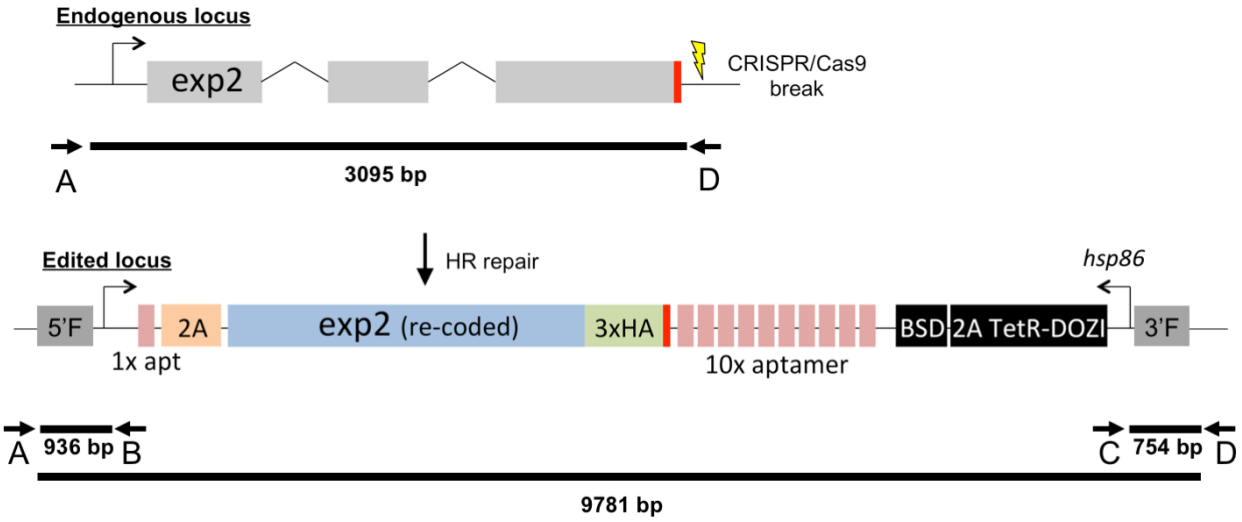

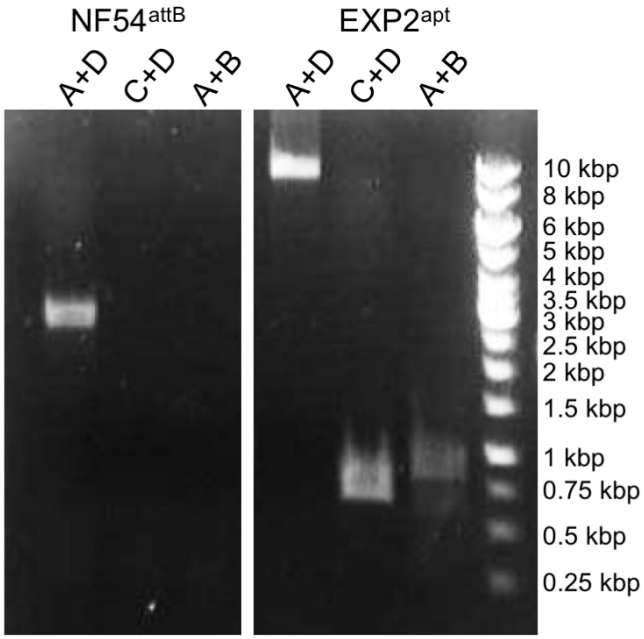

Supplementary Figure 1. Generation of EXP2^{apt} parasites. Schematic showing strategy for generation of conditional EXP2 knockdown parasites. CRISPR-Cas9 editing was employed to replace the endogenous *exp2* coding sequence in the NF54^{attB} strain with a recoded, 3xHA epitope tagged version of the gene flanked with an aptamer immediately upstream of the start codon and an array of ten aptamers immediately downstream of the stop codon. The integration donor also contained a cassette downstream of *exp2* for expression of a TetR-DOZI fusion and

the BSD selectable marker linked by the viral T2A skip peptide. Diagnostic PCR primers and expected amplicon sizes are shown for the locus before and after editing. Diagnostic PCR results for the parent NF54^{attB} and edited EXP2^{apt} parasites are shown. The experiment was performed once. Uncropped gels shown in Supplementary Fig. 12. 2A, thosea asigna virus 2A skip peptide; HA, haemagglutinin tag; BSD, blasticidin-S deaminase; TetR-DOZI, Tetracycline repressor-DOZI fusion; *hsp86*, *P. falciparum heat shock protein 86* promoter; kbp, kilobase pairs.

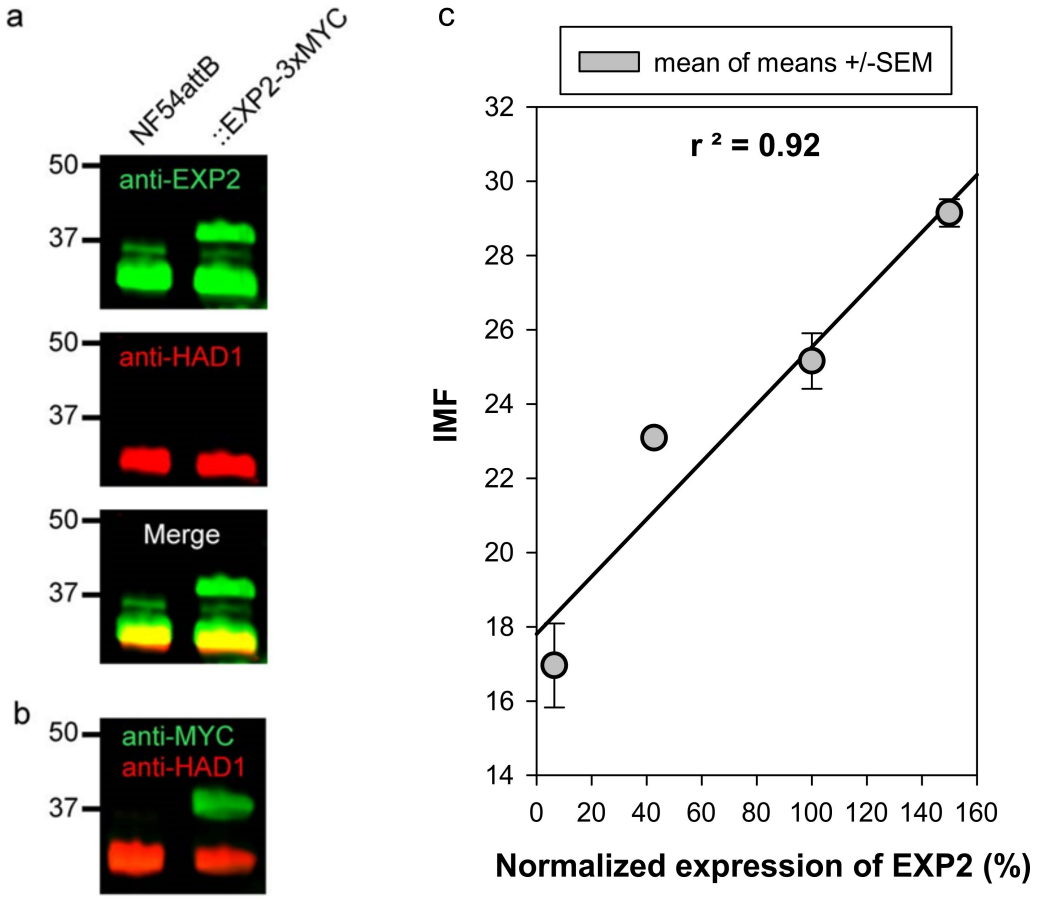

Supplementary Figure 2. Intraerythrocytic multiplication factor correlates with the level of EXP2 expression. a, b Western blot showing overexpression of EXP2 in NF54^{attB}:EXP2-3xMYC parasites bearing an additional copy of *exp2* with a C-terminal 3xMYC tag and expressed under the control of the *hsp86* promoter. Replicate blots were probed with anti-EXP2 (**a**) or anti-MYC antibodies (**b**). HAD1 serves a load control in both blots. Data are representative of two independent experiments. Uncropped western blots are shown in Supplementary Fig. 12. **c,** The number of merozoites produced per parasite expressed as the intraerythrocytic multiplication factor (IMF)[1] and the EXP2 expression level correlate with each other. N=3, 3, 3, 5 for ~10%, ~40%, 100% and ~150% normalized EXP2 expression, respectively. For the 10% data point, aTc was washed out 3-4 days prior to the experiment and

shows the IMF of the surviving and egressing parasites. Solid line shows linear regression of data.

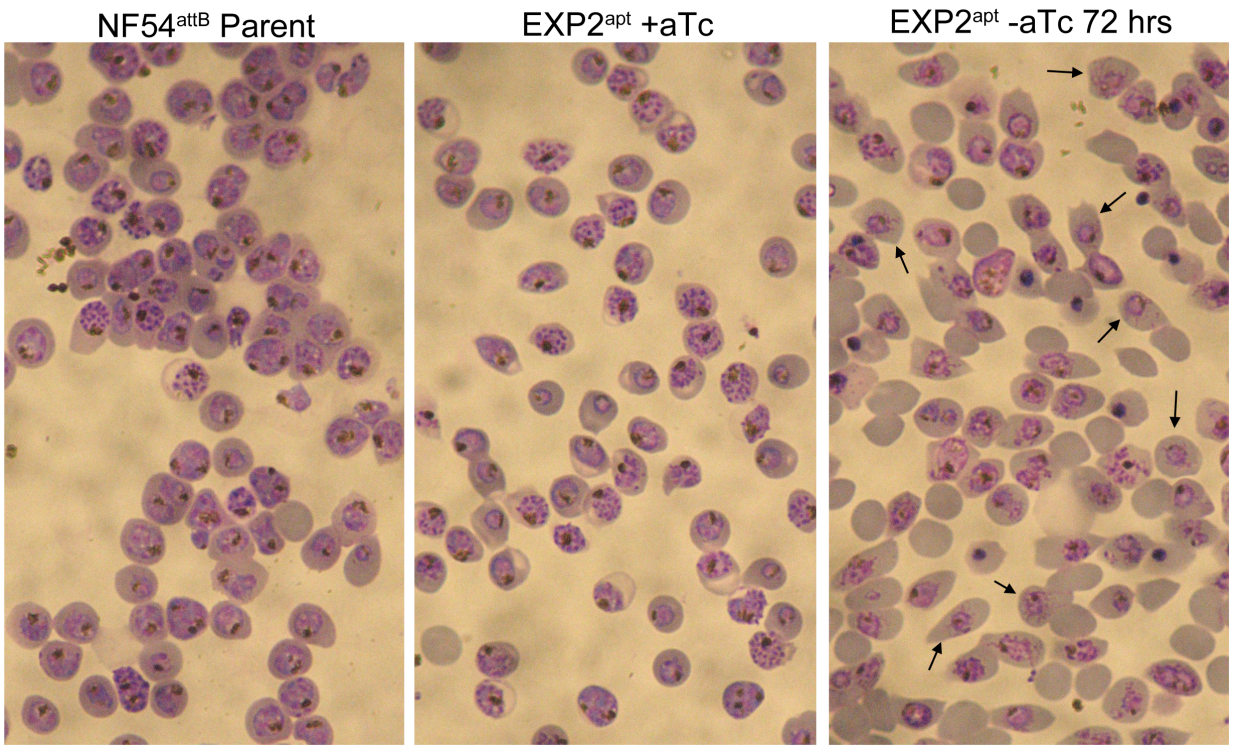

Supplementary Figure 3. EXP2 knockdown produces tubular PV distensions. a, EXP2^{apt} parasites were extensively washed to remove aTc and allowed to develop for 72 h ± aTc before trophozoite- and schizont-stage parasites were purified on a magnetic column. The NF54^{attB} parental line was purified in parallel as a control. Giemsa-stained thin smears show extensive protrusions from the periphery of EXP2^{apt} parasites following EXP2 knockdown (some prominent examples indicated by arrows). Images are representative of three independent experiments. Samples were used as input for transmission electron microscopy experiments shown in Fig. 1f. Scale bars are not available for these images. As a guide of scale, a typical human red blood cell has a diameter of 6-8 μm.

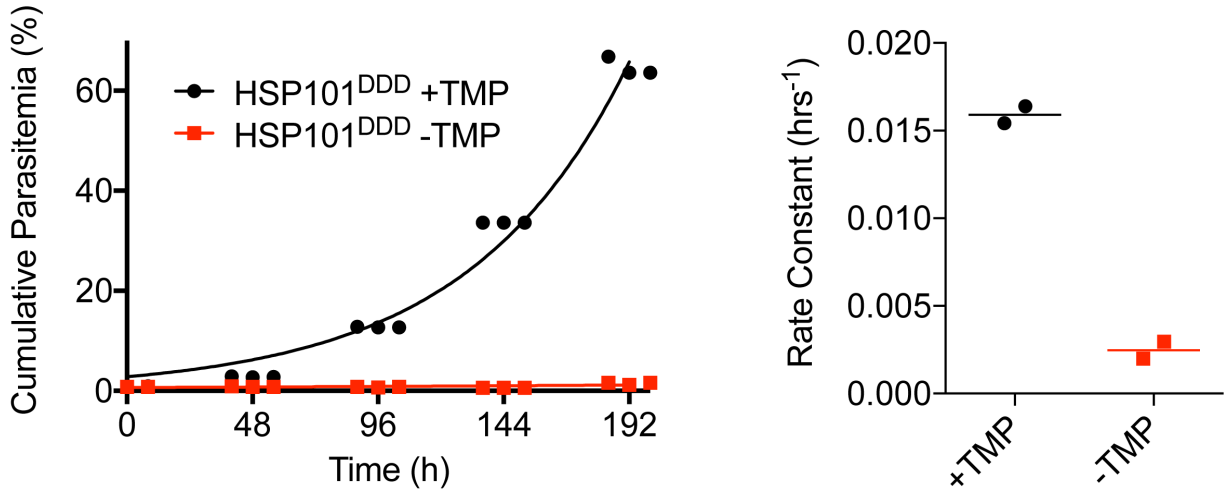

Supplementary Figure 4. Characterization of NF54^{attB}::HSP101^{DDD} parasites. Growth curve showing lethal growth inhibition upon TMP washout from NF54^{attB}::HSP101^{DDD} parasites as previously shown for the similar 13F10 and 14G11 lines generated in the 3D7 background[2]. Results from one experiment with three technical replicates are shown and are representative of two independent experiments. Dot plot shows exponential growth rate constant (hrs^{-1}) derived from the fit of two independent experiments and lines indicate means.

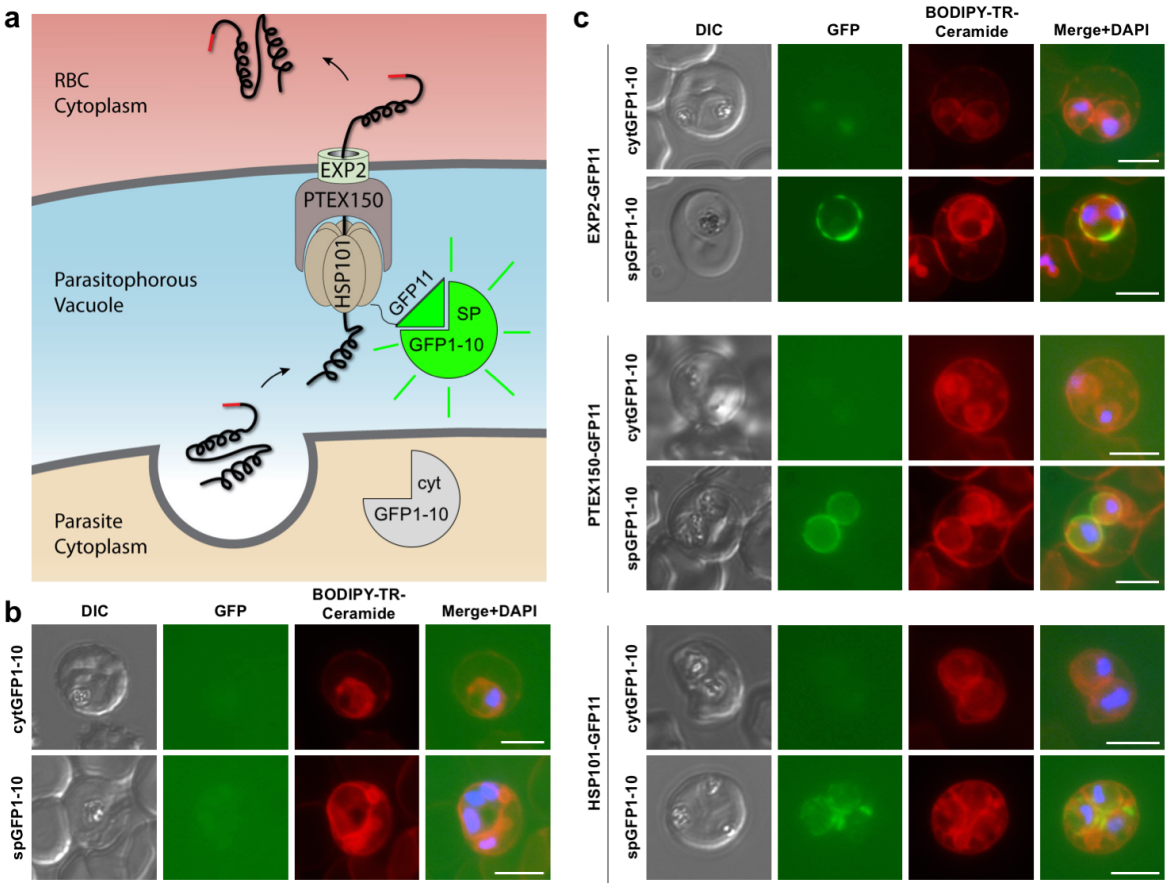

Supplementary Figure 5. Split GFP assays argue against export-dedicated subcompartments and resolve EXP2 topology. a, Schematic showing split GFP experimental design. GFP1-10 was targeted to the parasite cytosol (cytGFP1-10) or PV lumen (by N-terminal fusion of a signal peptide, spGFP1-10). Endogenous GFP11 tags were made in the cytGFP1-10 or spGFP1-10 parasite backgrounds on the C-terminus of EXP2, PTEX150 or HSP101 (schematic shows HSP101-GFP11 as an example). **b** Live fluorescence imaging of parasite lines expressing cytGFP1-10 or spGFP1-10. No appreciable GFP signal is observed. Infected RBCs were labeled with BODIPY-TR-Ceramide to demarcate the PVM and other membranes. **c,** Live fluorescence imaging of cytGFP1-10 and spGFP1-10 parasite lines bearing endogenous GFP11 tags on EXP2, PTEX150 and HSP101. Vacuolar GFP signal is observed in the spGFP1-10

parasite background but not in the cytGFP1-10 parasite background. All GFP channel images were acquired with equal exposure time. Data are representative of two independent experiments. DIC, differential interference contrast. Scale bars, 5 μm.

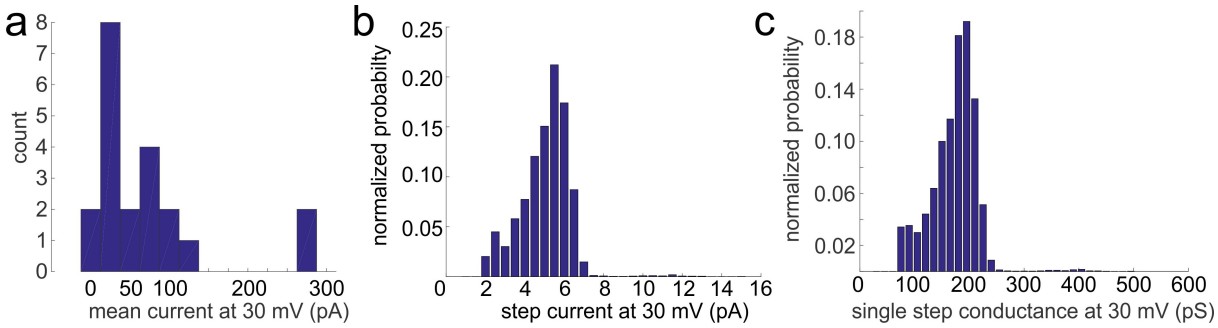

Supplementary Figure 6. Sub-conductances at 30 mV of the NF54^{attB} parent line. a, Histogram of the mean current of 22 patches at 30 mV. **b,** Histogram of current steps observed. The sum of the distribution of each recording was normalized to 1 before adding up the 22 patches into one histogram and renormalizing. **c,** Histogram of the observed sub-conductance step sizes calculated using the potential applied to the membrane. Normalization as in (**b**).

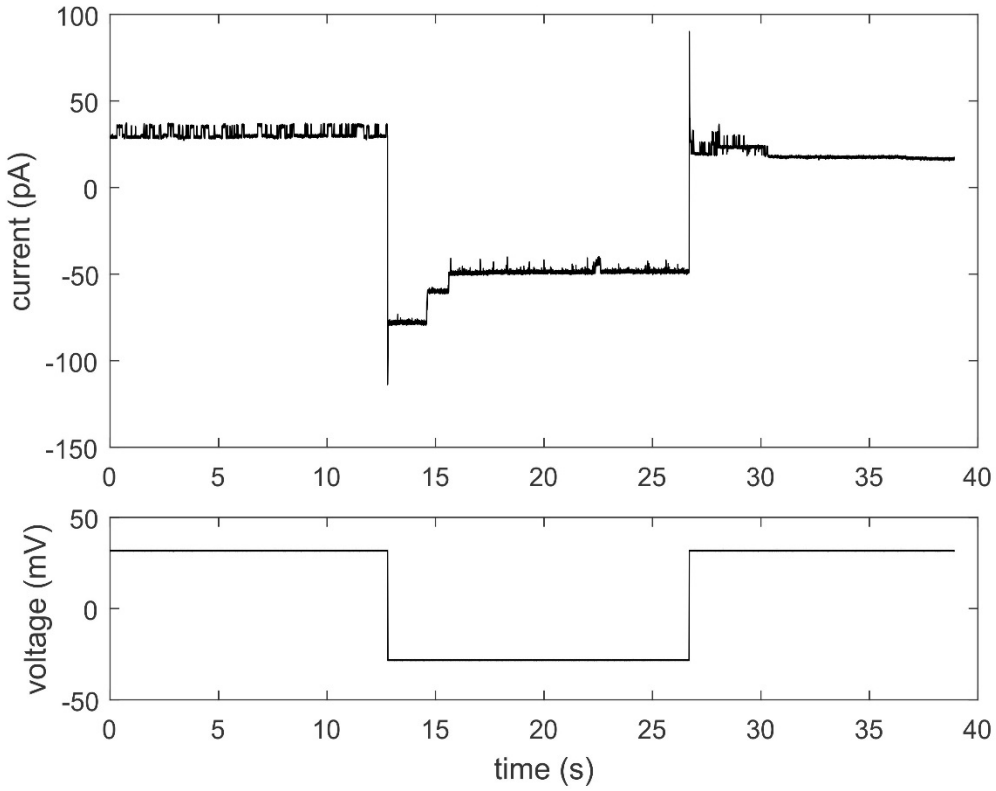

Supplementary Figure 7. Example of PVM channel rundown. Frequently, the channel activity (i.e. the total patch conductance and the frequency of stochastic channel opening and closing events at any chosen stable voltage) decreased over time during an experiment (termed 'channel rundown'). Rundown was observed similarly for all tested parasite lines (i.e. in a majority of the 85 experiments with channel activity reported in this work). The example chosen (recorded in an experiment with NF54^{attB}::EXP2-3xMYC) illustrates this rundown behavior. A decreased activity and lower current base line can be seen in the stretch at 27-40s when comparing to the stretch at 0-13s. Both stretches are recorded at 30 mV. In-between the voltage was switched to -30 mV, a voltage with normally little stochastic channel opening and closing events. 3 conductance steps were then resolved (293 pS, 317 pS [in a double step at 14.5 s] and 330 pS at 15.6s) that are larger than any of the stochastic steps observed regularly (compare to

Figure 3 and Supplementary Figures 6 and 8). We interpret those larger steps as channels leaving the membrane patch from which the recording is made and as the cause of the channel rundown, and on that basis we conclude that the PVM channel only partially closes with voltage.

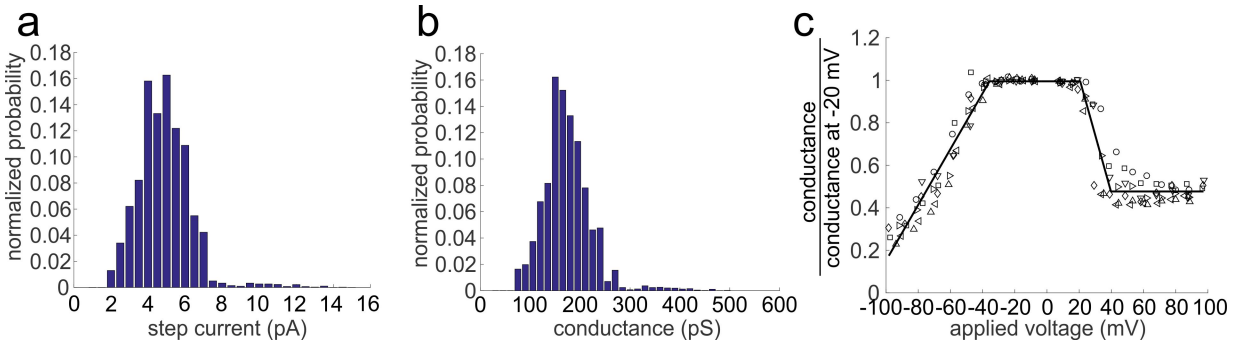

Supplementary Figure 8. HSP101^{DDD} 30 mV current step size and voltage response at 18 h after TMP washout. a, Histogram of current steps in the HSP101^{DDD} (-TMP 18 h) experiments. The sum of the distribution of each recording was normalized to 1 before adding up the 13 patches into one histogram and renormalizing. **b,** Histogram of the corresponding sub-conductance step sizes calculated using the potential applied to the membrane. Normalization as in **a**. **c,** Conductance-voltage of the HSP101^{DDD} line (-TMP 18 h). Different symbols denote individual experiments (N = 7). Solid line is a fit to the piecewise linear model (see methods). Fit parameters from individual fits: m_1=13.2±0.5 1/V, m_2=-29.2±4.4 1/V, $V_{half\ open,negative}$ = -55.8±1.1 mV, $V_{half\ open,positive}$ = 26.5±2.0 mV (mean±s.e.m.).

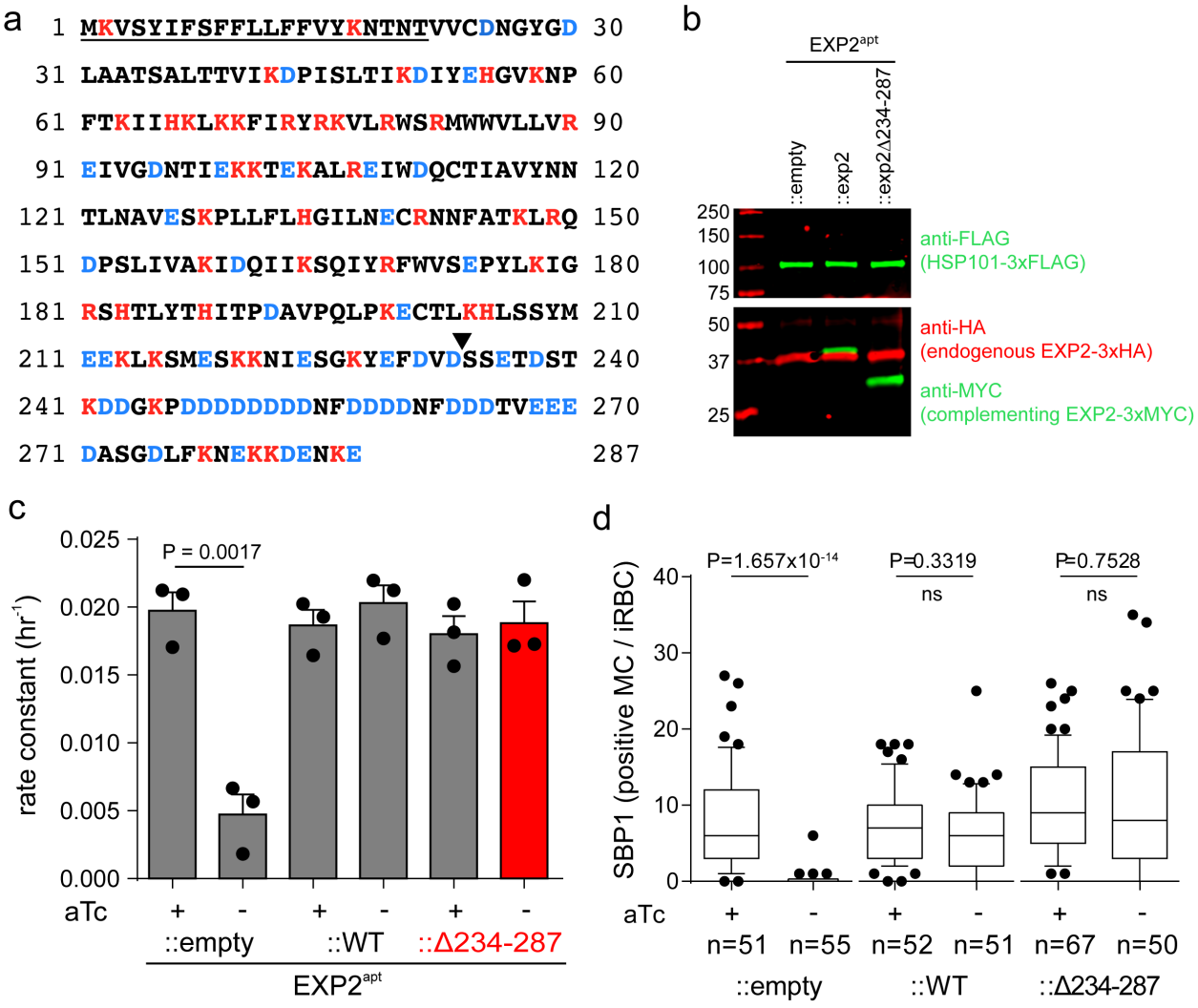

Supplementary Figure 9. Complementation of EXP2^{apt} with full length and C-terminally truncated versions of EXP2. a, EXP2 amino acid sequence with positively (red) and negatively (blue) charged residues indicated. Predicted signal peptide is underlined. Arrowhead indicates Δ234-287 truncation site. **b,** Western blot of EXP2^{apt}::HSP101-3xFLAG complemented with the empty vector, full length EXP2-3xMYC or EXP2Δ234-287-3xMYC. Predicted molecular weights after signal peptide cleavage: HSP101-3xFLAG, 102.9 kDa; endogenous EXP2-3xHA, 34.1 kDa; full length EXP2-3xMYC, 35.3 kDa; EXP2Δ234-287-3xMYC, 29.2 kDa. Data are representative of two independent experiments. Uncropped western blots are shown in Supplementary Fig. 12. **c,** Growth rate of EXP2^{apt} complemented lines +/- aTc. Mean

exponential growth rate constants (hr^{-1}) derived from the fit of three independent experiments are shown. Error bars indicate s.e.m. **d,** Quantification of IFA assays for SBP1 export in $EXP2^{apt}$ complemented lines. Data are pooled from two independent experiments, *n* is the number of individual parasite-infected RBCs. Boxes and whiskers delineate 25th-75th and 10th-90th percentiles, respectively. All *P* values determined by an unpaired, two-sided t-test.

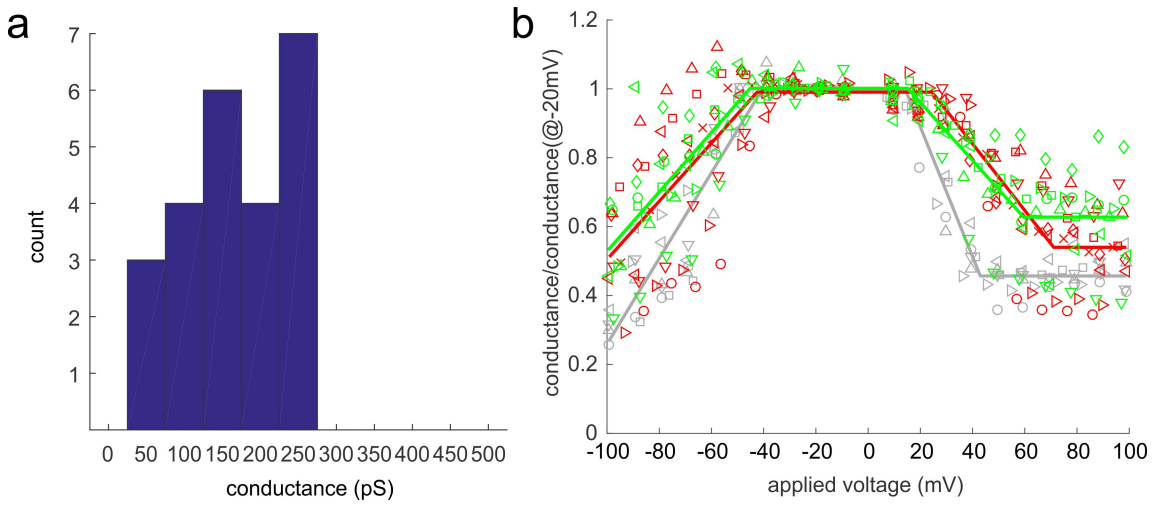

Supplementary Figure 10. EXP2^{apt}::Δ234-287 -aTc step size and conductance of EXP2^{apt}::Δ234-287 +aTc. a, Step-wise conductance found in the EXP2^{apt}::Δ234-287 parasite line -aTc. Step conductance was read off from traces recorded at 30 to 60 mV from 9 experiments. **b,** Conductance-voltage plot of EXP2^{apt}::Δ234-287 +aTc (green) in comparison with EXP2^{apt}::Δ234-287 -aTc (red) and the NF54^{attB} parent line (gray). Fit parameters from individual fits to the measurements of the +aTc condition: m_1=9.1±0.6 1/V, m_2=-8.8±1.8 1/V, $V_{half\ open,negative}$ = -67.2±3.3 mV, $V_{half\ open,positive}$ = 35.35±1.6 mV (mean±s.e.m.).

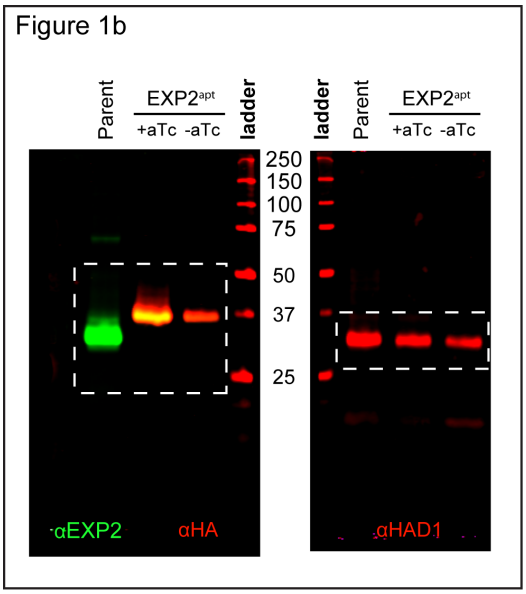

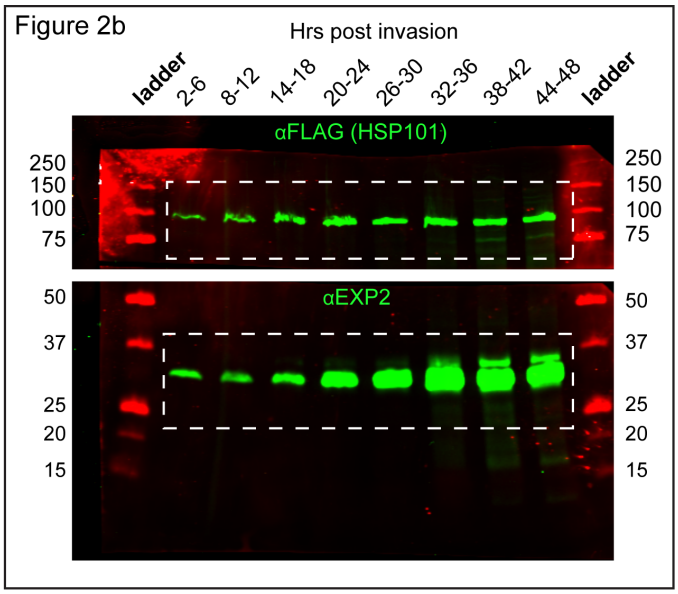

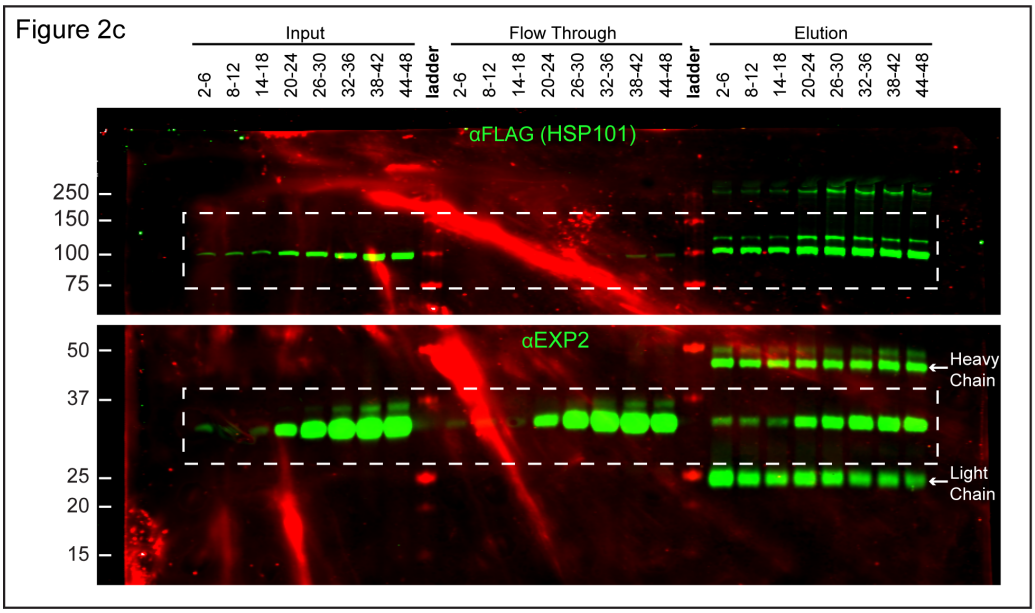

Supplementary Figure 11. Uncropped blots for main text figures 1b and 2b, c. Individual channels from two-color IR scans were converted to black and white for cropped, main text figures.

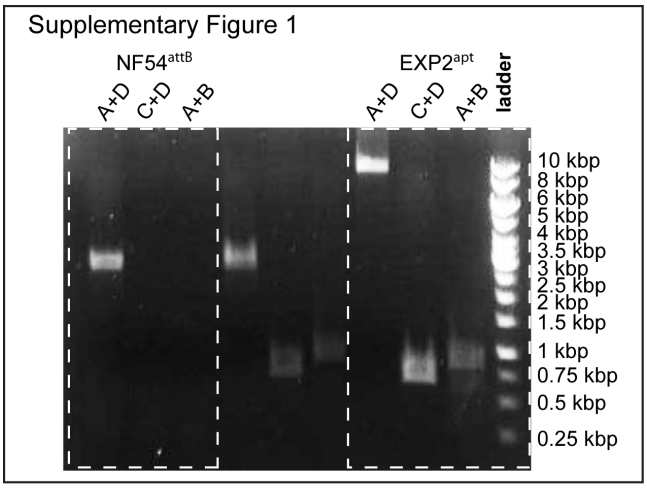

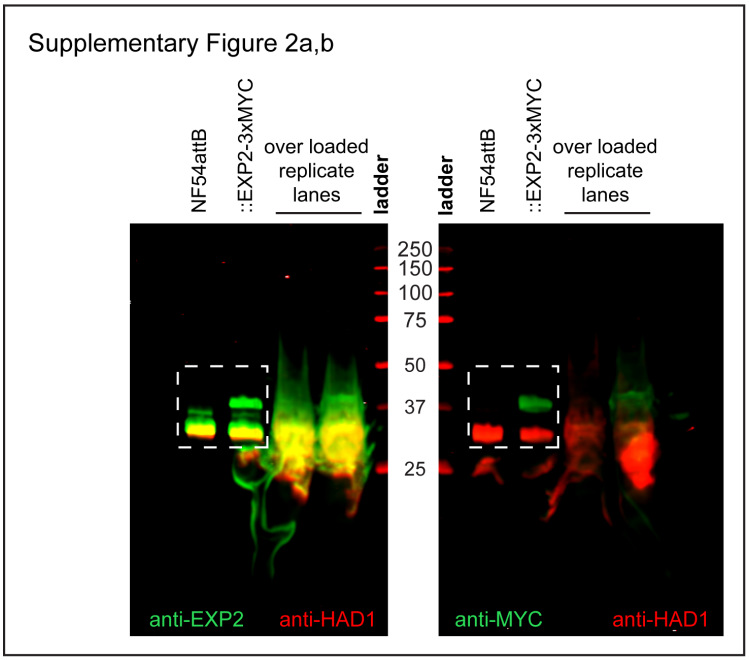

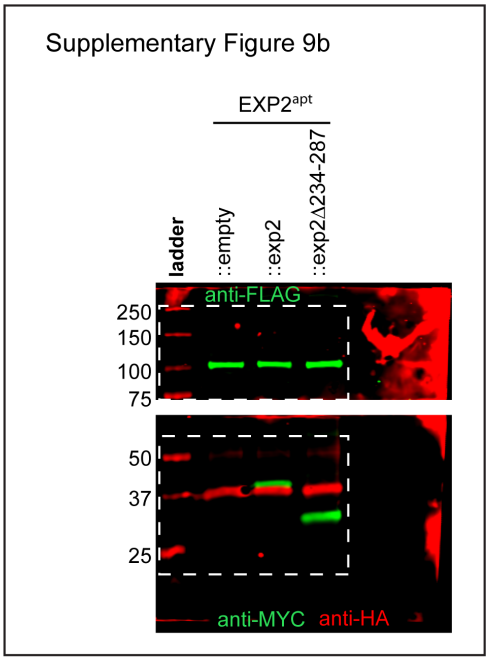

Supplementary Figure 12. Uncropped gels and blots for supplementary figures 1, 2a,b and 9b. For two-color IR scans in Supplementary Fig. 2a, b, individual channels are displayed.

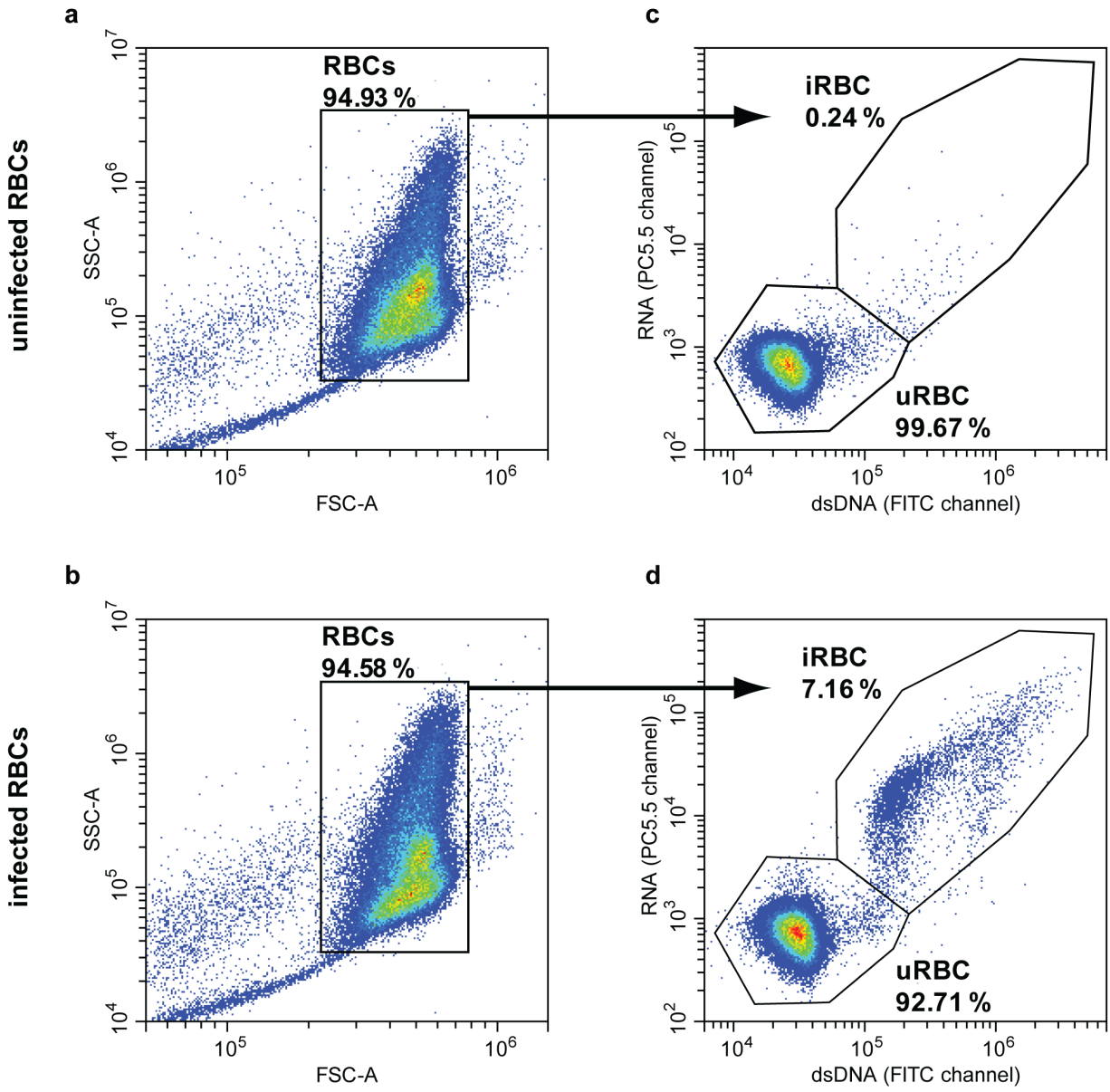

Supplementary Figure 13. Flow cytometry gating strategy. Sample data from uninfected and *P. falciparum*-infected RBC cultures stained with acridine orange are shown. **a, c** The RBC population was gated on a forward scatter (FSC)/side scatter (SSC) plot. Uninfected RBCs (uRBC) and parasite infected RBCs (iRBC) were gated by nucleic acid staining with acridine orange to detect dsDNA (FITC channel) and RNA (PerCP Cy5.5 channel).

Supplementary References

1 Glushakova, S. *et al.* Hemoglobinopathic erythrocytes affect the intraerythrocytic multiplication of Plasmodium falciparum in vitro. *The Journal of infectious diseases* **210**, 1100-1109, doi:10.1093/infdis/jiu203 (2014).

2 Beck, J. R., Muralidharan, V., Oksman, A. & Goldberg, D. E. PTEX component HSP101 mediates export of diverse malaria effectors into host erythrocytes. *Nature* **511**, 592-595, doi:10.1038/nature13574 (2014).